

## 論文内容の要旨

Studies on interactions of molecules with intense femtosecond laser pulses  
(高強度フェムト秒レーザーパルスと分子との相互作用に関する研究)

酒見 悠介

Interaction of a strong laser field with matter leads to many interesting phenomena such as high-order harmonic generation and nonsequential double ionization. The application of these phenomena includes attosecond pulse generation and tomographic imaging of molecular orbitals, and attracts scientists with various backgrounds (physics, chemical physics, biochemistry). The present study aims to reveal the dynamics of high-order harmonic generation with carrier-envelope phase (CEP) stabilized pulses (first part) and tunnel ionization from polar molecules (second part).

In the first part, we observe high-order harmonics generated with a CEP-stabilized driving pulse from the following four samples: N<sub>2</sub> aligned parallel to the laser polarization, N<sub>2</sub> aligned perpendicular to the laser polarization, CO<sub>2</sub> aligned parallel to the laser polarization, and randomly oriented CO<sub>2</sub>. As shown in figure 1, the spectra have small structures in the cutoff regions (the shortest wavelength region in high-order harmonic spectra), which change its shape depending on the value of the CEP. The small structures stem from the interference of attosecond pulses.

We Fourier analyze the spectra, and find that there are at least three peaks (Fourier components) in these Fourier spectra, specifically, at  $\Delta T = 1.35$  fs, 2.53 fs, and 3.88 fs for N<sub>2</sub> aligned parallel to the laser polarization. The values of  $\Delta T$  do not change as the CEP is varied, and the values do not change as molecular alignment condition is changed. The phase of the first Fourier component  $\phi_{\text{Fourier}}$  are independent of the value of the CEP, while the phases of the 2nd and the 3rd Fourier components,  $\phi_{\text{Fourier}}^{2\text{nd}}$  and  $\phi_{\text{Fourier}}^{3\text{rd}}$ , linearly increase as the value of the CEP is varied. These observations mean that in the observed spectra there exist at least three sinusoidal curves given by

$$\cos(\omega\Delta T_i + 2\phi_{\text{CEP}} + \phi_0 + \phi(\omega)), \quad (1)$$

where  $\phi(\omega)$  is a frequency dependent phase. By applying the inverse Fourier transform to the Fourier spectrum, we obtain these sinusoidal curves for each molecular sample. For CO<sub>2</sub>, in the suppressed region (42–54 eV) the phase of the 2nd and the 3rd Fourier peaks,  $\phi_{\text{Fourier}}^{2\text{nd}}$  and  $\phi_{\text{Fourier}}^{3\text{rd}}$ , are distorted, while outside the region these are relatively in phase.

We perform computational simulations to understand the underlying physics of the

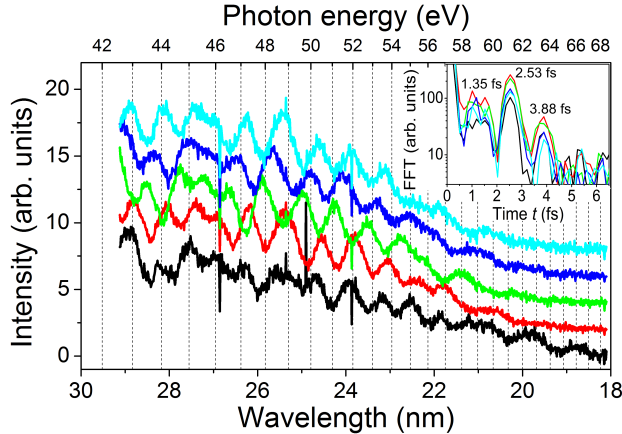


Figure 1: High-order harmonic spectra near the cutoff generated in parallel  $N_2$  for different values of CEP. The intensity of the probe pulse is estimated to be  $3 \times 10^{14}$  W/cm $^2$ . The values of the CEP are  $\pi/3$ ,  $2\pi/3$ ,  $\pi$ , and  $4\pi/3$  from the bottom to the top.

experimental results. We calculated the harmonics with a commonly used quantum mechanical model (the Lewenstein model) using the parameters that match the experimental conditions. The peaks in the computed spectra show shifts as a function of the CEP, which are similar to the experimental results. We analyzed the calculated spectra with the procedures used to analyze the experimental results. We obtain Fourier components at  $\Delta T = 1.15$  fs, 2.64 fs, and 3.96 fs. We find that the calculated Fourier spectra exhibit higher order components than the experimental results. The limited detector resolution and low signal-to-noise ratio may prevent these higher order Fourier components from being experimentally observed. The phase of the first Fourier component  $\phi_{\text{Fourier}}^{\text{1st}}$  does not depend on the value of the CEP, whereas the phases of the higher components show dependence on the value of the CEP as the experimental results.

In order to further discuss underlying physics in the experimental results, we carry out another simulation where a simple attosecond pulse train with harmonic chirp  $b$  is assumed. This simulation reveals that the introduction of the chirp  $b$  is essential to reproduce our experimental results. We compare the two chirps  $b$  obtained by the simple simulation and by a well-known relation. Taking into account uncertainties for the experimental parameters, we estimate the value of the chirp  $b$  to be  $1.1(\pm 0.5)$  fs $^{-2}$ . This value is in good agreement with the results  $0.6$  fs $^{-2}$  obtained by the simple model. This fact reinforces the interpretation of the observed fringes by the interference of attosecond pulses, and results in the possibility of observing the magnitude of the harmonic chirp  $b$  without direct measurements of the high-order harmonic phase.

Next we examine the possibility of observing the harmonic phase change in the harmonic spectra generated from aligned  $CO_2$  and  $N_2$  molecules. For aligned  $CO_2$  and  $N_2$  molecules, the harmonic phase depends both on the harmonic photon energy range and on the configurations of aligned molecules.

In the case of  $N_2$ , it is reported that HOMO-1 in addition to HOMO contributes to

the high-order harmonic spectra. Since the symmetry of HOMO-1 is  $\pi_u$ , the contribution from HOMO-1 to the harmonic spectra should be more significant in the perpendicular configuration, where the driving pulse polarization is perpendicular to the molecular axis of aligned molecules, than in the parallel configuration, where the driving pulse polarization is parallel to the molecular axis of aligned molecules. We also note apparent phase changes between the two configurations (parallel and perpendicular) or even the harmonic phase distortions at 43–46 eV in the harmonic spectral components from the second Fourier component. Although the observation of phase changes between the two configurations demonstrates the potential applicability of the present self-referencing interferometry to probe harmonic phase changes in the HHG from aligned molecules, we find that high-order harmonic spectra with better statistics, with which the harmonic spectral component from each Fourier component is evaluated, are necessary to ensure the quantitative reproducibility of the phase change and to point out a conclusive indication of the phase change.

In the case of CO<sub>2</sub>, destructive interference of electron de Broglie waves during the recombination process is successfully explained by the two-center interference picture. In fact, a  $\pi$  phase jump is observed in the harmonic photon energy range, where the harmonic intensity from aligned CO<sub>2</sub> molecules is suppressed, with various harmonic phase measurement techniques. One can see apparent phase changes or even anti-correlations in the harmonic phases between the two samples especially at 42–54 eV in the harmonic spectral component from the second Fourier component. However, since the intensities in the parallel configuration are very low, we find it rather difficult to provide a conclusive argument, and it should also be very difficult to apply the direct harmonic phase measurement techniques. We therefore emphasize that the strongly suppressed harmonic intensities in the parallel configuration should be further examined experimentally and theoretically as a new open question.

In the second part, we study the tunnel ionization dynamics of carbonyl sulfide by observing the molecular-frame photoelectron angular distributions (MF-PADs) correlated with ions (S<sup>+</sup>, CO<sup>+</sup>, CS<sup>+</sup>, and O<sup>+</sup>) produced from various photodissociation channels of carbonyl sulfide cations with an home-built coincidence velocity-map imaging spectrometer. In order to estimate the emitted direction of photoelectrons with respect to the molecular frame, we employ a coincidence measurement of a single electron and a single fragment ion. By using an elliptically polarized pulse, the ionization probability is much higher when the electric field directs in the direction of the major axis of the polarization ellipse. Assuming an instant dissociation, the direction of the momentum of fragment ions represents the direction of the target molecule, and with the help of the angular streaking technique, the ionization efficiency in the molecular frame can be obtained. We measured MF-PADs at four laser intensities  $5 \times 10^{13}$  W/cm<sup>2</sup>,  $1 \times 10^{14}$  W/cm<sup>2</sup>,  $1.5 \times 10^{14}$  W/cm<sup>2</sup>, and  $2.2 \times 10^{14}$  W/cm<sup>2</sup> with two polarization conditions of clockwise elliptical polarization and counterclockwise elliptical polarization, in both polarization cases ellipticity is set at  $\epsilon \sim 0.84$ . When the molecular axis is fixed to the  $z$  axis, the observed photoelectron images are regarded as the MF-PADs projected onto the  $xy$  plane.

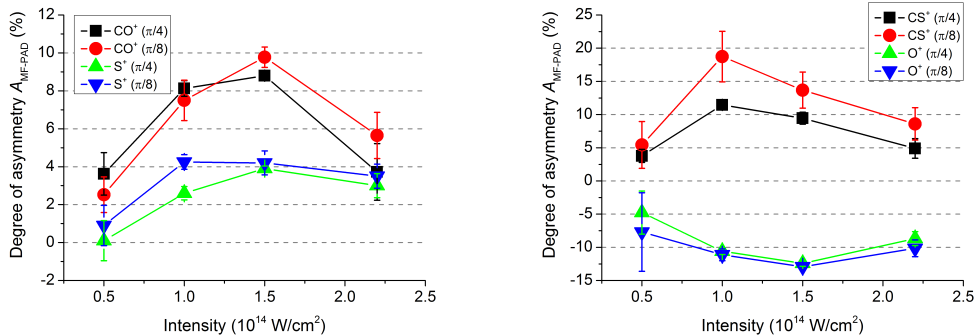


Figure 2: Degrees of asymmetry of MF-PADs  $A_{\text{MF-PAD}}$  for the S-loss dissociation cations ( $\text{CO}^+$  and  $\text{S}^+$ ) (left) and the O-loss dissociation cations ( $\text{CS}^+$  and  $\text{O}^+$ ) (right) as a function of the laser intensity. The two momentum distributions  $d_{\text{dis}}$  ( $\pi/4$  and  $\pi/8$ ) with respect to the major polarization axis are considered for each fragment.

The observed MF-PADs clearly have asymmetry in distribution along the momentum  $p_y$  depending on the polarization and the correlated fragment ions' momentum  $p_z$ . We define the degree of asymmetry  $A_{\text{MF-PAD}}$  of MF-PAD such that when  $A_{\text{MF-PAD}} > 0$ , electrons are more likely to be ionized from the O atom of OCS molecules than from the S atom of OCS molecules, and vice versa. Figure 2 shows the degrees of the asymmetry  $A_{\text{MF-PAD}}$  as a function of the laser intensity. As the intensity increases from  $5 \times 10^{13} \text{ W/cm}^2$  to  $1.0 \times 10^{14} \text{ W/cm}^2$  strong enhancements of the degree of asymmetry  $A_{\text{MF-PAD}}$  are observed for all fragments. The asymmetry  $A_{\text{MF-PAD}}$  also depends on the species of the fragment ions. Since the asymmetry reflects the angular-dependent ionization rates of OCS molecules, the observed asymmetry indicates that electrons are more likely to be ionized from the O atom than from the S atom for  $\text{S}^+$ ,  $\text{CO}^+$ , and  $\text{CS}^+$ , and vice versa for  $\text{O}^+$ . These observations mean that the dissociation processes and the tunnel ionization processes are correlated with each other, and the dynamics is sensitive to the laser intensity. We qualitatively discuss the mechanism by giving a hypothetical idea that the difference in the asymmetry depending on the correlated dissociation channels corresponds to the tunnel ionization of different (inner) molecular orbitals, leading to the difference in the (excited) states of the produced ions.